Self-Association of Lysozyme as Seen by Magnetic Relaxation Dispersion

Michael Gottschalk and Bertil Halle*

Department of Biophysical Chemistry, Lund University, SE-22100 Lund, Sweden

Received: March 1, 2003; In Final Form: May 14, 2003

The pH and salt dependent self-association of hen egg-white lysozyme (HEWL) has been studied extensively, mainly by scattering techniques, but it has proven difficult to distinguish oligomerization from long-range interactions. Because HEWL is the principal model system in studies of protein crystallization, it is important to establish its oligomerization behavior unambiguously. Here, we address this problem with the aid of proton magnetic relaxation dispersion (MRD), which can determine the sizes and populations of coexisting oligomers with minimal influence of long-range interactions. We find that HEWL is monomeric at pH 4 and dimeric at pH 9. Dimers as well as a higher oligomer are formed also at pH 4 in the presence of K_2SO_4. The dimer observed in solution has the same rotational correlation time as a dimer present in tetragonal HEWL crystals. The higher oligomer, consisting of about 16 HEWL monomers, is more abundant as the saturation limit is approached, but is suppressed by addition of sulfobetaine. It is also promoted by contaminating proteins, present in commercial HEWL preparations. These findings can explain why HEWL tends to form amorphous precipitates in the presence of sulfate and why crystallization of HEWL is facilitated by sulfobetaine. The MRD data also yield a residence time of 2 ns for several protein-associated water molecules, probably including the four-molecule cluster buried between the α and β subunits of HEWL.

Introduction

A molecular-level understanding of the mutual interactions of proteins in aqueous solution is a long-standing goal in biophysical chemistry.[1,2] Because this challenging problem has many ramifications, it has been addressed in several contexts. On the one hand, we would like to understand how proteins in the crowded intracellular environment[3,4] can recognize and selectively bind to receptors without being bogged down in unproductive associations. Closely related to this problem is the pathological aggregation of misfolded proteins.[5] On the other hand, the progress of crystallography-driven structural biology is vitally dependent on a supply of protein crystals that can be formed only by coaxing proteins into the intimate self-associations that they have been designed by evolution to avoid.

While our understanding of the nucleation, growth, and polymorphism of protein crystals is advancing rapidly,[6,7] we are still far from the ultimate goal of rational protein crystallization. To predict the optimal conditions for obtaining crystals of a particular protein amounts to specifying the protein concentration, pH, and temperature as well as the type and concentration of salts and other crystallizing agents. Such predictions must be based on a quantitative dissection of protein−protein interactions. The DLVO theory has enjoyed considerable success in the colloid field by modeling the interacting particles as smooth spheres with uniform surface charge and replacing the solvent by a dielectric continuum.[8] It is becoming increasingly clear, however, that a quantitatively useful description of protein−protein interactions must include atomic details, such as the discrete charge distribution[9,10] and the short-ranged, direct and solvent-mediated, interactions.[11,12]

Hen egg-white lysozyme (HEWL) has become the model system of choice for studies of protein crystallization. At least half a dozen crystal forms have been described and a variety of salts have been used as crystallizing agent.[13] However, the most common salting-out agent, ammonium sulfate, long proved ineffective for HEWL crystallization, producing instead amorphous precipitates or gels.[14] Only recently has it been shown that HEWL crystals grow (slowly) from concentrated solutions of high-purity HEWL in the presence of $(NH_4)_2SO_4$ or other sulfate salts.[15] Furthermore, nondetergent sulfobetaines (NDSBs) were found to suppress the formation of amorphous precipitate, thus facilitating HEWL crystallization from sulfate solutions.[16] The ternary phase diagram of the system HEWL−H_2O−$(NH_4)_2SO_4$ has now also been mapped out, revealing a rich phase polymorphism,[17] including a liquid−liquid phase transition.[18−20]

Protein self-association enters at two stages in the crystallization process. At the nucleation stage, a cluster of protein molecules of critical size assemble in solution, and in the growth phase, protein molecules attach to the crystal faces. Although proteins are usually crystallized from highly supersaturated solutions, the protein−protein interactions that are responsible for crystallization may be manifested also in undersaturated solutions. Indeed, the osmotic second virial coefficient, measured in dilute protein solutions, has turned out to be a useful indicator of solution conditions conducive to protein crystallization.[21] The critical nucleus may be a transient aggregate induced by critical concentration fluctuations,[22] but it is also conceivable that a stable oligomer, present already in undersaturated solutions, is required to form a nucleus with the proper intermolecular geometry. Such oligomers may also be the building blocks for crystal growth. This scenario has been proposed for tetragonal HEWL crystals, where oligomers that already possess the 4_3 helix symmetry of the crystal are thought to be involved in the nucleation and growth phases.[23] Furthermore, it has recently been shown that the compact decamers that build up the low-pH crystal forms of bovine pancreatic trypsin inhibitor (BPTI) are present as stable species in solution, even far below

* Corresponding author. Telephone: +46-46-2229516. Fax: +46-46-2224543. E-mail: bertil.halle@bpc.lu.se.

10.1021/jp034527k CCC: $25.00
Published on Web 07/11/2003

saturation.[24,25] Analysis of protein−protein contacts in crystals suggests that such preformed crystal oligomers may not be rare.[26]

HEWL has long been known to undergo reversible self-association at pH >5, forming dimers and, in more concentrated solutions or above pH 9, also higher oligomers.[27,28] In recent years, self-association of HEWL as a function of pH, salt concentration, and protein concentration (in the undersaturated and supersatured regimes) has been extensively studied by a variety of techniques, including static and dynamic light scattering,[29−33] small-angle neutron[33−36] and X-ray[37,38] scattering, dialysis kinetics,[39] and self-diffusion.[40−42] All of these methods face the fundamental problem of distinguishing stable protein oligomers from long-range interactions among monomers and/or oligomers. In view of this ambiguity, much of the published data have been interpreted either by assuming ideal solution behavior and attributing all effects to oligomerization, or by assuming negligible concentrations of stable oligomers and ascribing all effects to interactions among monomers. The latter point of view, i.e., that scattering data (as well as other data that reflect solution nonideality) do not provide evidence for stable HEWL oligomers in undersaturated solutions, has been advocated by several groups.[33,37,43] It has even been concluded that oligomers are absent at salt concentrations near the point of salting-out precipitation[30] and during crystal growth.[38] The picture is further clouded by the influence of impurities (commercial HEWL preparations may contain as much as 5% (w/w) contaminating proteins[44]) and buffers (typically present at concentrations of 100 mM).

Protein oligomers can be unambiguously identified, with little or no influence of long-range interactions, by monitoring the rotational diffusion of the protein. (For example, the long-ranged Coulomb repulsion involving the protein net charge may retard translational diffusion substantially, but, for symmetry reasons, it cannot affect protein rotation.) In the case of HEWL, this has been done by depolarized light scattering,[45] ^{15}N NMR relaxation,[46] and fluorescence depolarization.[47] Only the latter study was aimed at self-association. Although a modest increase in the rotational correlation time was observed on addition of salt at pH 4.6, no inferences were made about the population or size, or even the existence, of stable oligomers.[47]

More detailed information about protein oligomerization can be obtained by measuring the magnetic relaxation dispersion (MRD) of the water ^{1}H resonance. This technique has been used primarily to study protein hydration,[48,49] but it can also provide information about self-association. Under favorable conditions, the relaxation dispersion profile, which typically extends over four frequency decades, yields the rotational correlation times and relative populations of all coexisting oligomeric species. Large oligomers can be detected even at low (<1%) populations, and the method is independent of the association−dissociation kinetics. Because the rotational correlation time is insensitive to long-range interactions, it reflects the true oligomerization state. We have recently used the MRD method to study the BPTI decamer[25] and the dimer and octamer of β-lactoglobulin.[50] Water ^{1}H MRD[51−56] data as well as water ^{2}H MRD[51,55,57] and ^{17}O MRD[57,58] data from HEWL solutions have been reported by several groups. Only one of these studies[54] dealt with self-association, but the MRD data did not extend above 50 MHz and were analyzed with the aid of an expression that has subsequently been shown[59] to be physically inconsistent.

Here, we present ^{1}H MRD data extending from 10 kHz to 200 MHz from HEWL solutions at pH 4 and 9 and at different concentrations of K_2SO_4. These data provide conclusive evidence for the presence of a HEWL dimer at pH 9 and at pH 4 in the presence of salt. By analyzing the available crystal structures, we identified a potential solution dimer in the tetragonal space group. The rotational correlation time calculated by molecular hydrodynamics for this crystal dimer agrees quantitatively with the experimental correlation time. In the presence of salt, we also find a higher oligomer. The formation of this species is suppressed by addition of zwitterionic sulfobetaine and by removal of the contaminating proteins in the most widely used commercial HEWL preparation.

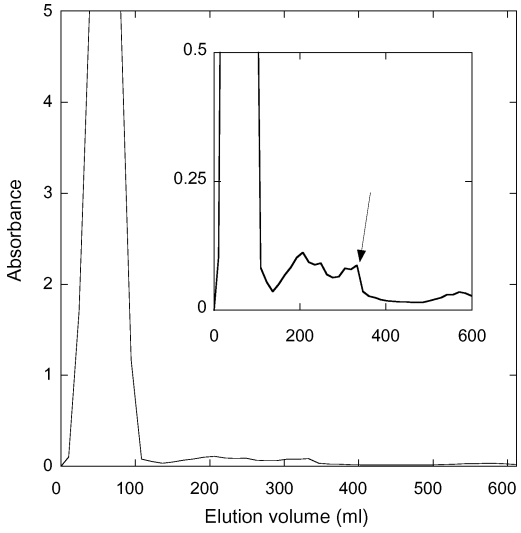

Figure 1. Elution profile of HEWL from a DEAE-Sephacel column. The arrow in the inset shows the region containing ovalbumin and ovotransferrin.

Experimental Section

Protein Purification. Hen egg-white lysozyme (HEWL) was obtained from Sigma (Catalog No. L-6876, Lot No. 65H7025) as a three times crystallized, dialyzed, and lyophilized powder. This preparation was further dialyzed to remove any salt, twice against deionized water and twice against Millipore water. The protein was then repurified by anion exchange chromatography at pH 8.8 (10 mM Tris buffer) on a 22 mm diameter DEAE-Sephacel column, eluted with a NaCl gradient (0−0.5 M). Apart from the main HEWL peak, the chromatogram showed a tail with several minor peaks (see Figure 1). For MRD samples, the fractions corresponding to the main peak were collected, dialyzed as described above, and lyophilized. The purity of the HEWL fraction was checked by agarose gel electrophoresis (20 mg ml^{-1}) and SDS-PAGE, confirming the absence of the two negative bands observed with HEWL that had not been chromatographically purified. SDS-PAGE identified these bands as ovalbumin (66 kDa) and ovotransferrin (78 kDa), as previously found in HEWL from Sigma.[44] SDS-PAGE on the purified HEWL fraction showed a band corresponding to a (covalent) HEWL dimer. This was presumably formed by disulfide interchange in the gel, since the MRD data at pH 4 and without added salt showed no sign of HEWL dimers (see below).

Preparation of MRD Samples. MRD measurements were performed on chromatographically purified protein as well as on protein that only had been dialyzed. In either case, the lyophilized protein was dissolved in Millipore water or in oxygen-depleted water (<0.001% O_2, Fluka BioChemika). The pH was adjusted by microliter additions of HCl or NaOH. No buffers were used. Potassium sulfate (>99.9%, BDH) and/or

the nondetergent sulfobetaine 3-(1-pyridino)-1-propanesulfonate (>97%, Fluka), with trade name NDSB 201, were dried in a desiccator and then added to the protein solution. The solution was centrifuged at 14000*g* for 3 min to remove a small fraction of aggregated material. Protein concentrations were determined spectrophotometrically (Shimadzu UV-1601) at 280 nm using an extinction coefficient of 2.64 mL mg^{-1} cm^{-1}, determined from quantitative amino acid analysis. To remove paramagnetic oxygen, the solution was gently bubbled with argon gas for 4 h, whereupon the 10 mm NMR tube was sealed with a septum. To remove paramagnetic ions, the NMR tubes had been left with 3 M HCl for 24 h and then carefully rinsed with Millipore water and EDTA solution. With this procedure, the ^{1}H relaxation rate in a pure water sample was found to agree with the standard literature value[60] of 0.266 s^{-1}, and remained within 1% of this value for at least 10 days.

Relaxation Dispersion Measurements. The longitudinal relaxation of the water ^{1}H resonance was measured from 10 kHz to 200 MHz using (1) a Stelar Spinmaster fast field-cycling (FC) spectrometer (10 kHz−12 MHz); (2) a field-variable iron-core magnet (Drusch) equipped with a Tecmag Discovery console (10−78 MHz); and (3) Bruker Avance DMX 100 and 200 spectrometers with conventional cryomagnets (100.1 and 200.1 MHz). The temperature was maintained at 27.0 ± 0.1 °C using a Stelar variable temperature control unit (below 100 MHz) or a Bruker Eurotherm regulator (at 100 and 200 MHz). Temperatures were checked using a thermocouple referenced to an ice−water bath.

The longitudinal relaxation rate R_1 was measured with the inversion recovery method (fixed-field experiments) and by the prepolarized (<4 MHz) or nonpolarized (>4 MHz, avoiding short evolution times) field-cycling protocols (FC experiments). The small contribution from nonexchanging protein protons was eliminated by selective integration (fixed field) or by delayed acquisition (FC). All other details of the relaxation experiments were as previously described.[25] The accuracy in R_1 (one standard deviation) is estimated to ±1% at the two highest fields and 1−2% at the other fields.

Analysis of Relaxation Dispersion Data. The measured ^{1}H relaxation rate is due to thermal fluctuations of intramolecular and intermolecular magnetic dipole−dipole couplings experienced by water protons and labile HEWL protons in fast or intermediate exchange (residence time < 10 ms, typically) with the water protons.[48,49] The relaxation dispersion, i.e., the frequency dependence of R_1, is produced by long-lived (residence time 10^{-9}−10^{-2} s) water molecules in intimate association with the protein and by labile protons with residence times in the same range. The dispersion profile, $R_1(\omega_0)$, from a solution containing HEWL in several different oligomeric states is described by the following relations:[48,49]

$$R_1(\omega_0) = \alpha + b_0 \langle L(\omega_0,\tau_0)\rangle + \sum_n b_n L(\omega_0,\tau_n) \qquad (1)$$

$$L(\omega_0,\tau_n) = \frac{0.2\tau_n}{1+(\omega_0\tau_n)^2} + \frac{0.8\tau_n}{1+(2\omega_0\tau_n)^2} \qquad (2)$$

Here, b_n and τ_n are the mean-square fluctuation amplitude and the correlation time associated with the *n*th dispersion step. The correlation time τ_n is related to the HEWL oligomer rotational correlation time $\tau_{R,n}$ and the mean proton residence time $\tau_{H,n}$ as[48]

$$\frac{1}{\tau_n} = \frac{1}{\tau_{R,n}} + \frac{1}{\tau_{H,n}} \qquad (3)$$

Labile protons generally have residence times much longer than the protein rotational correlation time and therefore do not affect τ_n. This is usually the case also for protons in deeply buried internal water molecules. However, water molecules in deep surface pockets or trapped in large internal cavities may have site residence times in the range 1−10 ns [50,61,62] and will then shorten the correlation time τ_n according to eq 3. All our MRD profiles from HEWL solutions show a dispersion step with a correlation time of about 2 ns, attributable to such water molecules. This contribution is modeled by the second ($n = 0$) term in eq 1, which, for simplicity, is represented by a single correlation time. Our main focus here is on the dispersion steps $n = 1$, 2, or 3 that report on the oligomeric species of HEWL (monomer, dimer, or higher oligomer). The correlation time τ_n can be identified with the isotropic rotational correlation time τ_R of the *n*th oligomer species, and the amplitude b_n allows its fractional population to be determined. Note that we use the index *n* to identify the oligomer species. The sum in eq 1 therefore contains only those terms that correspond to the species actually present (in detectable amounts) in the sample. At pH 4 and 0.3 M K_2SO_4, for example, the tri-Lorentzian ($N = 3$) dispersion profile is a weighted superposition of dispersion components associated with water exchange ($n = 0$), dimer rotation ($n = 2$), and higher oligomer rotation ($n = 3$), with no contribution from monomers ($n = 1$).

In the analysis of MRD data, we actually used a more involved dispersion function, which is a linear combination of the intramolecular dispersion function in eq 2 and an intermolecular dispersion function.[48] The relative weight of the intermolecular function was set to 0.33,[63] but any value in the allowed range 0−1 could be used without significantly affecting the correlation times and amplitudes deduced from the fits. The parameter α in eq 1 represents all frequency-independent contributions to the measured relaxation rate, including bulk water, rapidly exchanging ($\tau_H \ll 1$ ns) surface waters, and the secular (zero-frequency) intermolecular contribution from internal waters and labile HEWL protons.[63] Because of incomplete characterization of the highest frequency dispersion step (with a correlation time of about 2 ns), the α parameter could not be determined with useful accuracy in all cases. The dispersion profiles are therefore displayed with the small frequency-independent contribution subtracted and with the frequency-dependent part normalized to the same HEWL concentration:[25]

$$R_1^{\,\mathrm{norm}} = (R_1 - \alpha)N_T / N_T^{\,\mathrm{norm}} \qquad (4)$$

where N_T is the number of water molecules per HEWL monomer in the solution, calculated from the concentration C_P (in mM), specific volume $\bar{\nu}_P = 0.702$ cm^3 g^{-1}, and molar mass $M_P = 14{,}314$ g mol^{-1} of the protein, the density $\rho_W = 0.9965$ g cm^{-3} of water (at 300 K) as $N_T = (10^6/C_P - \bar{\nu}_P M_P)\rho_W/18.02$. N_T^{norm} was taken as 9400, corresponding to a HEWL monomer concentration of 5.56 mM.

The experimental relaxation dispersion data were subjected to nonlinear Marquardt−Levenberg χ^2 minimization[64] with the model function given by eqs 1 and 2. This fit involves the $2N + 1$ parameters α, b_n, and τ_n, with the products $b_n\tau_n$ constrained to be nonnegative. The number *N* of Lorentzians to be included in the fit was determined objectively by the *F*-test with a cutoff probability of 0.9.[59,64] The dispersions were thus found to be

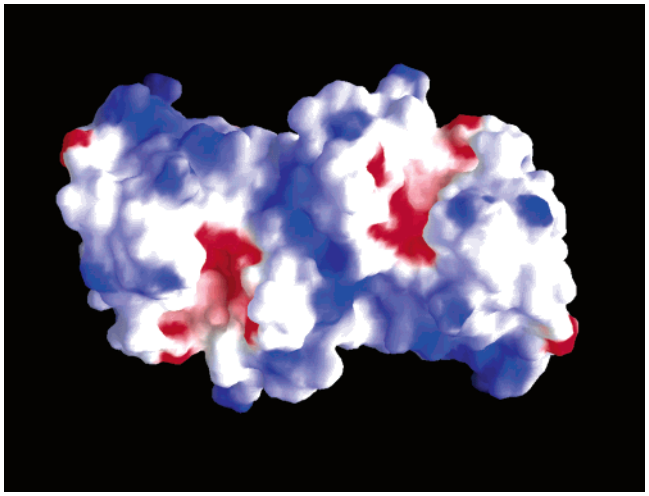

Figure 2. Dimer with 560 Å^2 buried surface area per monomer, present in tetragonal HEWL crystals. The depicted dimer was generated from the coordinates of the 1.33 Å resolution crystal structure 193L.[70] The surface, rendered with GRASP,[77] maps the electrostatic potential on a scale from −5 (red) to +11 k_BT/e (blue), calculated with dielectric constants of 4 (protein) and 78 (solvent), no salt, and full structural charges.

adequately modeled by two or three Lorentzians ($N = 2$ or 3), including the 2 ns water dispersion ($n = 0$). Quoted uncertainties in the fitted parameter values correspond to one standard deviation and were obtained by the Monte Carlo method[64] using 1000 synthetic data sets.

Hydrodynamic Calculations on Crystal Dimer. To obtain a plausible model for the HEWL dimer, we searched 50 X-ray structures of wild-type HEWL in apo form for extensive crystal contacts that might stabilize a dimer also in solution. This analysis was carried out on the Protein Quaternary Structure (PQS) server at the European Bioinformatics Institute (http://pqs.ebi.ac.uk), which generates all crystal dimers by applying the symmetry operations of the space group to the single HEWL molecule in the asymmetric unit and then computes the surface area buried in the dimer interface. The search produced one potential solution dimer, present in 28 crystals belonging to the tetragonal space group $P4_32_12$ and with a C_α root-mean-square deviation of only 0.33 ± 0.13 Å relative to the dimer in the structure 193L. In forming this dimer, each monomer buries 560 Å^2 (9%) of its solvent-accessible surface area (1.4 Å probe radius). The contact region, located near the "top" of the β domain and on the opposite side to the catalytic cleft (see Figure 2), involves no ionizable side chains. Two symmetry-related water molecules are buried in the dimer interface, each involved in strong hydrogen bonds to both monomers.

The crystal dimer was used as structural model for hydrodynamic calculations of the rotational correlation time of the HEWL dimer. The program HYDROPRO v. 5a[65] was used to compute the rotational diffusion tensor $\mathbf{D}_R$ of the HEWL monomer and dimer from eight crystal structures of HEWL in space group $P4_32_12$ (PDB codes 193L, 1HEL, 1RFP, 1IO5, 1LSA, 1LYZ, 2LYZ, and 1DPX). In these calculations, each non-hydrogen atom in the crystal structure is replaced by a spherical bead of radius a_H. The shell of beads remaining after all internal beads have been deleted is then filled with smaller spheres of radius σ that act as point sources of hydrodynamic friction. The rotational diffusion tensor $\mathbf{D}_R$ is computed as a function of σ and extrapolated to $\sigma = 0$.[66] The rank-2 isotropic rotational correlation time is defined as $\tau_R = (2\mathrm{Tr}\mathbf{D}_R)^{-1}$. Because macroscopic continuum hydrodynamics is not strictly valid on the atomic scale, this calculation does not necessarily yield the true τ_R. The approach usually adopted is to regard the bead radius a_H as an empirical parameter (rather than using the van der Waals radii of the actual atoms), the value of which is determined by requiring that the calculation agrees with the experimental value of a particular hydrodynamic quantity, such as τ_R.[65] In our calculations, a_H was fixed to 3.26 Å, which makes the calculated τ_R (for the 0.95 Å resolution monomer structure 4LZT) agree with the value $\tau_R = 6.9 \pm 0.2$ ns (scaled to the viscosity of pure H_2O at 300 K) determined by ^{15}N NMR relaxation.[46] With this radius, we obtained τ_R(dimer)/τ_R(monomer) = 2.3 ± 0.1 for all eight crystal structures. This value, which coincides with the result for the β-lactoglobulin dimer,[50] is intermediate between the value 2.75 for two touching spheres[66] and the value 2.00 for spherical dimer and monomer. For a general asymmetric top, the dispersion function (or spectral density) involves five rotational correlation times. The rotational anisotropy, defined as the ratio of the longest and shortest of these five correlation times, is 1.27 for the HEWL monomer and 1.48 for the dimer (crystal structure 1HEL). These anisotropies are too small to produce significant deviations from spherical top behavior in the MRD profile. Accordingly, we describe both monomer and dimer with single (isotropic) rotational correlation times.

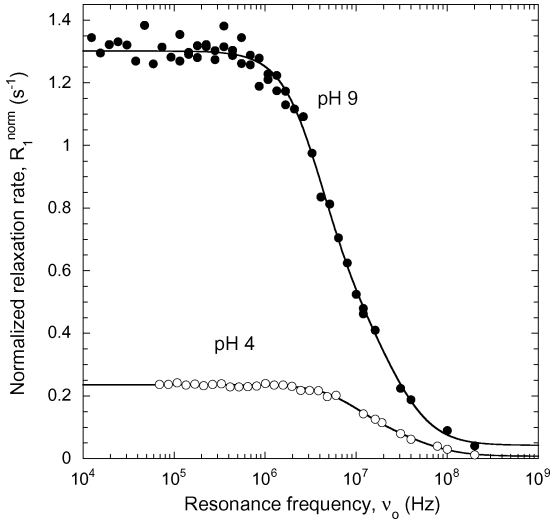

Figure 3. ^{1}H relaxation dispersion profiles from aqueous solutions of chromatographically purified HEWL at 27 °C and pH 4.0 or 9.0. The data have been normalized to 5.56 mM HEWL. The dispersion curves resulted from fits according to eqs 1 and 2 with $N = 2$.

Results and Discussion

Assignment of Correlation Times. We consider first MRD data obtained from salt-free HEWL solutions. The most striking effect of raising pH from pH 4 to 9 is a 5-fold increase of the dispersion amplitude (see Figure 3), to a roughly equal extent resulting from slowing of protein rotational diffusion and from base-catalyzed exchange of labile HEWL protons (see below). Unconstrained fits to these dispersion profiles according to eqs 1 and 2 require two correlation times at either pH value (see Table 1 and Experimental Section). The number N of Lorentzian terms included in eq 1 was determined by the F-test (see Table 2 and Experimental Section). The shortest correlation time, corresponding to τ_0 in eq 1, is significantly shorter than the rotational correlation time of the HEWL monomer and is therefore assigned to protein-associated water molecules with residence times of 2−3 ns (see eq 3).

The other correlation time is a factor 2.5 ± 0.4 longer at pH 9 than at pH 4, matching the rotational correlation time ratio

TABLE 1: Results of Fits to ^{1}H MRD Data from HEWL Solutions at 300 K

			τ_n[a]/ns				b_n[b]/10^7 s^{-2}			
pH	C_{salt}/M	C_P/mM	$n=0$	$n=1$	$n=2$	$n=3$	$n=0$	$n=1$	$n=2$	$n=3$
4.0	0	5.56	1.7 ± 0.6	8.7 ± 1.3			4.5 ± 1.0	1.9 ± 0.5		
4.0	0.30	5.49	1.9 ± 0.3		17.5 ± 1.2	115 ± 8	6.2 ± 0.8		1.8 ± 0.1	0.11 ± 0.01
4.0	0.50	5.69	2.2 ± 0.4		18.2 ± 1.2	120 ± 8	4.2 ± 0.6		1.9 ± 0.1	0.18 ± 0.02
9.0	0	5.42	3.5 ± 0.3		21.8 ± 1.3		11.9 ± 0.4		4.1 ± 0.5	

[a] Correlation times include the effect of salt-induced viscosity enhancement. [b] Dispersion amplitudes have been normalized to $C_P = 5.56$ mM (or $N_T = 9400$).

TABLE 2: Statistics for the MRD Fits in Table 1

pH	C_{salt}/M	N[a]	$\chi_r^2(N)$[b]	F_N[c]	P_N[d]	P_{N+1}[d]
4.0	0	2	0.90	2.3	0.99	0.60
4.0	0.30	3	0.79	4.0	1.00	0.63
4.0	0.50	3	0.85	5.2	1.00	0.50
9.0	0	2	1.62	3.8	1.00	0.84

[a] Total number of Lorentzian terms in eq 1 (including the $n = 0$ component). [b] Reduced chi-square merit function, defined as in ref 59. [c] F-test statistic, $F_N = \chi_r^2(N)/\chi_r^2(N-1)$. [d] P_N is the probability that the MRD data represent a dispersion with N, rather than $N-1$, Lorentzian components.

τ_R(dimer)/τ_R(monomer) $= 2.3 \pm 0.1$ predicted by molecular hydrodynamics calculations on crystal structures (see Experimental Section). We thus assign these correlation times to the HEWL monomer (pH 4) and dimer (pH 9). The correlation time $\tau_1 = 8.7 \pm 1.3$ ns obtained at pH 4 agrees reasonably well with the result $\tau_{R1} = 6.9 \pm 0.2$ ns (viscosity scaled to pure H_2O at 300 K) derived from ^{15}N NMR relaxation[46] (4 mM HEWL, pH 3.8, no salt). Somewhat shorter correlation times (viscosity scaled to H_2O) have been obtained from ^{2}H MRD (5.8 ± 0.3 ns) and ^{17}O MRD (4.3 ± 0.5 ns) on HEWL at pH 4.4 and 300 K.[57,58] These correlation times, however, were derived from single-Lorentzian fits and therefore correspond to a weighted average of τ_0 and τ_1. In conclusion, the MRD data are consistent with a complete monomer → dimer transition between pH 4.0 and 9.0, but do not exclude a modest polydispersity at either pH. On the other hand, the MRD data clearly rule out a significant population of substantially larger oligomers at either pH 4 or 9. Although the pH 9 correlation time τ_2 agrees closely with the rotational correlation time computed for the dimer present in tetragonal HEWL crystals, it does not prove that this particular dimer structure exists in solution. Because τ_R depends more strongly on volume than on shape, any compact dimer structure formed by association of two native HEWL monomers would give a τ_R value close to the observed one.

Assignment of Dispersion Amplitudes. Although not essential for extracting information about self-association, the mean-square fluctuation amplitudes b_n ($n \geq 1$) are of some interest as they are proportional to the number of protons (per HEWL monomer) with residence times long enough ($\tau_{H,n} > \tau_{R,n}$) to sample the rotational diffusion of the oligomer but short enough ($\tau_{H,n} < x_n/(b_n\tau_{R,n})$, with x_n the fractional population of species n) to act as a relaxation sink for the observed water ^{1}H magnetization.[48,49] The water and labile proton contributions to ^{1}H MRD data are not easily separated,[63] but ^{17}O MRD reports exclusively on long-lived water molecules. A reanalysis of the published ^{17}O MRD data,[57] using a bi-Lorentzian dispersion function with τ_0 and τ_1 taken from the present study (and scaled to the viscosity of D_2O) yields $N_1S_1^2 = 1.1 \pm 0.1$ for the product of the number of long-lived ($\tau_H \gg 10$ ns) water molecules and their mean-square orientational order parameter. Ignoring any difference between the ^{17}O and ^{1}H order parameters,[48] and assuming the same relative contribution from intermolecular dipole−dipole couplings as for the internal waters in BPTI,[63] we find that this translates into a water contribution to b_1 of 1.0×10^7 s^{-2}. The b_1 value obtained from the fit to the ^{1}H MRD data at pH 4 is twice as large (see Table 1), but the difference can be accounted for by HEWL protons in hydroxyl and carboxyl groups with the expected pK_a values[67,68] and proton exchange rate constants.[69] The substantial increase of b_2 at pH 9 (see Table 1) can be attributed to base-catalyzed exchange of lysine and arginine side-chain NH protons[69] and should not be significantly affected by dimerization.

Inspection of high-resolution crystal structures of HEWL reveals five potentially long-lived water molecules, all with zero solvent-accessible surface area, low thermal B factors, and extensive hydrogen bonding to the protein.[57] Four of these are located in a large cavity (three of them mutually hydrogen bonded) between the α and β domains, and the fifth one is buried in a small cavity at the "top" of the β domain. A buried sodium ion coordinates two partly buried water molecules,[70] but since ^{23}Na MRD measurements (K. Snoussi, unpublished results) indicate that the ion is short-lived, this should also be the case for these two water molecules. Our reanalysis of the ^{17}O MRD data[57] indicates that HEWL may contain only one long-lived water molecule. If this is the singly buried water molecule, the four-water cluster must have shorter residence times and may account for much of the τ_0 dispersion. This assignment is supported by recent molecular dynamics (MD) simulations.[71]

The parameter α in eq 1 yields an estimate of the product of the number N_S of water molecules in contact with the protein surface and their relative dynamic retardation, $\rho_S = \tau_S/\tau_{bulk} - 1$.[48,49] (We neglect the small contribution to α from internal motions of labile HEWL protons.[72]) The fits to the MRD data in Figure 3 yield $N_S\rho_S = 2100 \pm 200$ at pH 4 and 2300 ± 200 at pH 9, close to the values previously derived from ^{2}H and ^{17}O MRD on HEWL.[57,58] With $N_S \approx 500$,[73] the ^{1}H MRD results yield $\rho_S \approx 4.4$, as for most other globular proteins[57] and in agreement with recent MD simulations on HEWL.[73]

Salt-Induced Self-Association. The addition of K_2SO_4 to a HEWL solution at pH 4 greatly increases the dispersion amplitude (see Figure 4), but the effect is smaller than that seen on going to pH 9 (Figure 3). This is because the amplitude parameters b_n are now unaffected (see below) so that the entire effect is due to the slower rotational diffusion of salt-induced oligomers. A comparison of Figures 3 and 4 clearly shows that salt addition gives rise to a new dispersion step with a correlation time (τ_3) much longer than that for the dimer (τ_2). In the presence of salt, three correlation times are thus needed to fit the MRD data (see Tables 1 and 2). To improve the accuracy of the dispersion amplitudes b_2 and b_3, and the oligomer fractions derived from them, we fitted the two MRD profiles

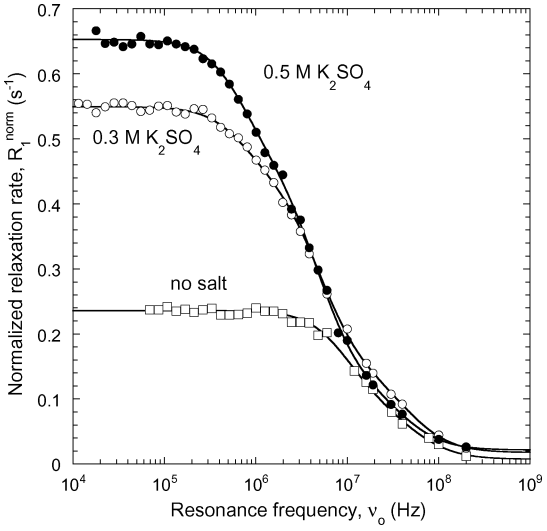

Figure 4. ^{1}H relaxation dispersion profiles from aqueous solutions of chromatographically purified HEWL at 27 °C and pH 4.0 in the absence of added salt and in the presence of 0.30 or 0.50 M K_2SO_4. The data have been normalized to 5.56 mM HEWL. The dispersion curves resulted from fits according to eqs 1 and 2 with $N = 2$ or 3.

from salt-containing solutions jointly with τ_2 and τ_3 constrained to be the same in the two solutions. In other words, we assume that the same oligomers are present in both cases, but with different relative populations. In performing this joint fit, we took into account the salt-induced enhancement of the bulk solvent viscosity (6% for 0.3 M and 10% for 0.5 M K_2SO_4).

As in the absence of salt, we find a correlation time $\tau_0 \approx 2$ ns, attributed to the exchange of buried water molecules (see above). The intermediate correlation time, corrected to the viscosity of pure H_2O, is $\tau_2 = 16.5 \pm 1.1$ ns, which agrees even more closely than at pH 9 (see above) with the dimer rotational correlation time $\tau_{R2} = 6.9 \times 2.3 = 15.9$ ns obtained by scaling the monomer correlation time from ^{15}N NMR relaxation[46] by the dimer/monomer correlation time ratio from molecular hydrodynamics (see Experimental Section). The viscosity-corrected long correlation time is $\tau_3 = 109 \pm 7$ ns, a factor 16 ± 1 longer than the monomer rotational correlation time τ_{R1}. We assign the correlation time τ_3 to a higher HEWL oligomer. If this oligomer has a compact structure, so that the rotational correlation time is proportional to its volume, then the correlation time ratio, $\tau_3/\tau_{R1} = 16$, should be close to the aggregation number. While the MRD data thus indicate the presence of an oligomer formed by association of about eight dimers, they cannot exclude a certain amount of polydispersity in the population of large oligomers.

Having assigned the dispersion components to oligomeric species, we now proceed to determine their relative populations from the mean-square fluctuation amplitudes b_2 and b_3 given in Table 1. These amplitudes can be expressed as $b_n = x_n\beta_n$, where x_n is the fraction of HEWL molecules that belong to the nth oligomer species or, equivalently, the weight fraction of that species.[25] The intrinsic mean-square fluctuation amplitude β_n is proportional to the number of protons (per HEWL monomer) with residence times long enough to sample the rotational diffusion of the oligomer but short enough to act as a relaxation sink for the observed water ^{1}H magnetization. We assume that the number of internal water molecules and rapidly exchanging labile hydrogens contributing to the observed dispersion are unaffected by self-association at pH 4. The fractional populations can then be obtained as $x_n = b_n/B$, where $B = b_1 + b_2 + b_3$ is the amplitude sum. If this assumption is correct, B should be independent of the oligomer fractions (at a given pH). As seen from Table 3, this is the case.

The MRD data indicate that the monomer → dimer transition is complete already at 0.3 M K_2SO_4. On increasing the salt concentration to 0.5 M, the fraction of higher oligomer increases slightly at the expense of the dimers. Because coexisting monomers and dimers are not seen in any of the investigated samples, we cannot determine the monomer → dimer association constant K. However, the absence of a detectable monomer population at $C_P = 5.5$ mM indicates that $K > 10^3$ M^{-1} in 0.3 M K_2SO_4. Whereas a small population of monomers coexisting with a larger population of dimers can hardly be detected by MRD, large oligomers can easily be detected even at low populations because the dispersion amplitude is proportional to the relative oligomer population x_n as well as to the oligomer volume (via τ_{Rn}). We can therefore rule out, under all investigated conditions (also at pH 9), the presence of oligomers much larger than 16-mers. We can also rule out a broad distribution of large oligomers, as implied by an isodesmic indefinite association model.[40,41,74]

Most previous studies of salt-induced self-association of HEWL have used NaCl, the most common salting-out agent for HEWL. Under our conditions (5.5 mM HEWL, pH 4.0, 300 K), the solubility limit (with respect to crystallization of HEWL) is about 0.35 M NaCl.[75] The solubility of HEWL is higher in sulfate salts, but 0.5 M K_2SO_4 should be close to the solubility limit.[15,17] At pH 4.0, HEWL carries a net charge of about +12.[67,68] The main effect of salt may be to screen the Coulomb repulsion, thereby allowing two HEWL monomers to approach closely enough for the attractive short-range interactions to come into play. Because the Debye length is as short as 3.2 Å in 0.3 M K_2SO_4, screening of long-range repulsion should be essentially complete already at the lower salt concentration. At pH 9, the net charge is only half as large and so the Coulomb repulsion is reduced by a factor 4. This scenario contrasts with that observed for BPTI, where self-association (to a decamer) sets in at higher salt concentration, with a dominant monomer population remaining even at 0.9 M NaCl.[25] In the BPTI decamer, however, a large number of positively charged side chains are clustered together in a narrow channel. The effect of counterions therefore cannot be described by the linear Debye−Hückel theory.[25] The stronger salt dependence observed here indicates that the HEWL dimer does not involve a similar charge concentration. The crystal dimer (see Figure 2), which may or may not be identical to the solution dimer, has no ionic residues at all in the dimer interface. Even if linear Debye screening can account for much of the salt effect on HEWL dimerization, the marked dependence of HEWL solubility on salt type[7,13] (and not just on ionic strength) shows that this cannot be the whole story. Presumably, a similar dependence exists for self-association.

Scattering studies have produced divergent conclusions about salt-induced self-association of HEWL (see Introduction). The main reason for the lack of consensus is probably the widely adopted (but unjustified) assumption of solution ideality.[43] In a small-angle X-ray scattering study,[37] which found no evidence for self-association in the presence of a range of monovalent salts even at very high (up to 1 M) salt concentrations (well above the saturation limit for ~1 mM HEWL), it was concluded that "polydisperse oligomers" are formed in the presence of 0.5 M $(NH_4)_2SO_4$ (1.4 mM HEWL, pH 4.5, 18 °C). It was suggested that these oligomers are responsible for the formation of amorphous precipitate, rather than crystals, in the presence of sulfates. The oligomers identified in the X-ray study may well

TABLE 3: Oligomer Fractions in HEWL Solutions at 300 K

				$100x_n$ /%		
pH	C_{salt} /M	C_P /mM	B^a /10^7 s^{-2}	$n = 1$	$n = 2$	$n = 3$
			Purified HEWL Preparation			
4.0	0	5.56	1.9 ± 0.5	1		
4.0	0.30	5.49	1.9 ± 0.1		94.4 ± 0.6	5.6 ± 0.6
4.0	0.50	5.69	2.1 ± 0.1		91.5 ± 0.9	8.5 ± 0.9
9.0	0	5.42	4.1 ± 0.5		1	
			Crude HEWL Preparation			
4.0	0	5.52	2.8 ± 1.1	99.3 ± 0.8		0.7 ± 0.8
4.0	0.30	5.45	2.5 ± 0.3		93.8 ± 1.2	6.2 ± 1.2
4.0	0.50	5.59	2.4 ± 0.2		90.0 ± 1.5	10.0 ± 1.5
4.0	$0.50 + 0.50^b$	5.45	2.0 ± 0.3		96.9 ± 2.1	3.1 ± 2.1
9.0	0	5.80	7.0 ± 0.4		96.6 ± 0.7	3.4 ± 0.7

[a] Sum of dispersion amplitudes ($n = 1-3$) normalized to $C_P = 5.56$ mM (or $N_T = 9400$). [b] This sample contained 0.50 M K_2SO_4 and 0.50 M NDSB 201.

be of the same nature as the higher oligomer found here in the presence of K_2SO_4. In contrast, a dynamic light scattering study[30] found a linear decrease of the collective diffusion coefficient with HEWL concentration up to 1.4 mM HEWL in 1 M $(NH_4)_2SO_4$ (pH 4, 25 °C), which was taken to imply the absence of self-association. However, interaction effects may have masked a weak nonlinearity. That such interaction effects are present even at high salt concentrations is evident from the greatly increased slope of diffusion coefficient versus C_P on going from 1.00 to 1.33 M $(NH_4)_2SO_4$ (see Figure 3a in ref 30).

Effect of Protein Impurities. During the course of this study, we found that contaminating proteins, mainly ovalbumin and ovotransferrin, present in the commercial HEWL preparation used here have a small but significant influence on the self-association behavior. The contaminating proteins were therefore removed by anion exchange chromatography (see Experimental Section). All MRD data discussed so far were obtained with this repurified protein batch. In the following, we refer to the two protein batches as the crude and purified protein. (Note that also the "crude" protein was exhaustively dialyzed; see Experimental Section.)

To illustrate the effect of protein contamination, we show in Figures 5 and 6 MRD profiles measured under conditions matching those in Figures 3 and 4, but with the crude protein. In all cases, the low-frequency relaxation rate is significantly higher for the crude protein than for the purified protein. Performing the fits as before, we find that the correlation times do not differ significantly from those obtained with the purified protein (viscosity-corrected $\tau_2 = 15.4 \pm 1.0$ ns and $\tau_3 = 108 \pm 9$ ns), but the amplitudes and associated oligomer fractions are slightly different (see Table 3). Specifically, the higher oligomer is more abundant for the crude protein under all investigated conditions. Even in the absence of salt, at least at pH 9, we now find a small population of higher oligomers. The species responsible for the longest correlation time (τ_3) cannot be monomers of the contaminating proteins ovalbumin and ovotransferrin, which should have shorter rotational correlation times (30−40 ns) and are expected[44] to be present at concentrations an order of magnitude lower than the higher oligomer that we see at pH 9.

If, as discussed above, the higher oligomer promotes the formation of amorphous precipitate, then protein purity may have been an issue in the many failed attempts to crystallize HEWL with the aid of sulfate salts.[14] Significantly, when HEWL ultimately was crystallized from a variety of sulfate salts (at pH values in the range 4−8), it had undergone elaborate repurification (including cation exchange chromatography).[15]

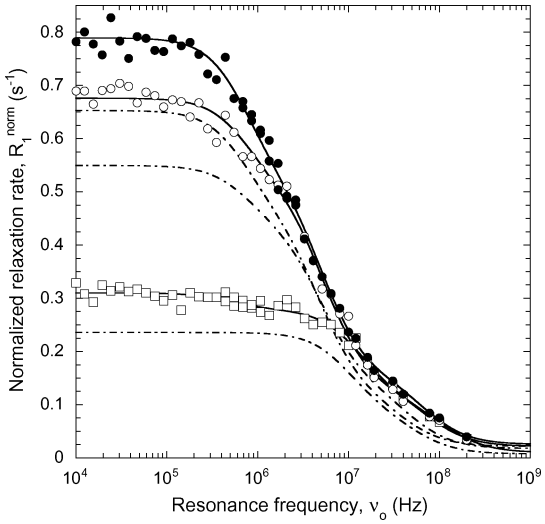

Figure 5. ^{1}H relaxation dispersion profiles from aqueous solutions of "crude" HEWL at 27 °C and pH 4.0 in the absence of added salt and in the presence of 0.30 or 0.50 M K_2SO_4. The symbols have the same meaning as in Figure 4. The data have been normalized to 5.56 mM HEWL. The dispersion curves resulted from fits according to eqs 1 and 2 with $N = 2$ or 3. The dashed curves, taken from Figure 4, refer to chromatographically purified HEWL.

Dispersal of Higher Oligomers by Sulfobetaine. The first successful attempt at crystallizing HEWL from sulfate solution at acidic pH used 0.9 M $(NH_4)_2SO_4$ in combination with 0.5 M of the nondetergent sulfobetaine *N*,*N*,*N*-dimethylethylammonium-1-propanesulfonate (NDSB 195).[16] The authors hypothesized that the zwitterionic sulfobetaine acts by preventing amorphous aggregation that would otherwise interfere with crystallization. To test this hypothesis, we performed MRD measurements on HEWL in 0.5 M K_2SO_4 to which also 0.5 M of the sulfobetaine 3-(1-pyridino)-1-propanesulfonate (NDSB 201) had been added. As seen from Figure 6, the sulfobetaine strongly suppresses the relaxation rate at low frequencies. From the fit to these data, we find that the three correlation times are the same (within the experimental uncertainty) as in the absence of sulfobetaine, whereas the amplitudes differ. Specifically, we see a 3-fold reduction of the fraction higher oligomer, but the dimer does not appear to dissociate into monomers (see Table 3). This supports the hypothesis[16] that sulfobetaines act by suppressing the formation of large oligomers. A possible mechanism might be that the aromatic ring and propyl chain of NDSB 201 associate with nonpolar regions on the protein surface and that the hydration (or dielectric stabilization) of the positive nitrogen and negative sulfonate group prevents these regions from coming into hydrophobic contact. Such a mech-

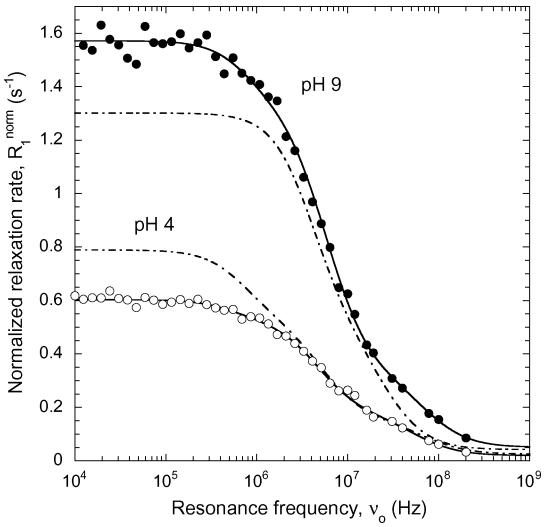

Figure 6. The two upper ^{1}H relaxation dispersion profiles refer to aqueous solutions of "crude" (data points, solid curve) or chromatographically purified (dashed curve, from Figure 3) HEWL at 27 °C and pH 9.0 in the absence of added salt. The two lower ^{1}H relaxation dispersion profiles refer to aqueous solutions of "crude" HEWL at 27 °C and pH 4.0 containing 0.50 M K_2SO_4 and 0.50 M sulfobetaine NDSB 201 (data points, solid curve) or just 0.50 M K_2SO_4 (dashed curve, from Figure 5). The data have been normalized to 5.56 mM HEWL. The dispersion curves resulted from fits according to eqs 1 and 2 with $N = 2$ or 3.

anism is also consistent with the ability of NDSBs to prevent aggregation in the early stages of protein folding.[76]

Previous ^{1}H MRD Studies of HEWL. The only previous MRD study to address the problem of HEWL self-association reports ^{1}H MRD profiles at pH 4, 7, and 9 for 1.3 mM HEWL at 4 °C in the presence of 0.15 M KCl and an unspecified amount of phosphate buffer.[54] The authors analyzed their data with the aid of an empirical dispersion function, which has subsequently been shown to be devoid of physical significance.[59] Due to a combination of experimental scatter and lack of data above 50 MHz, the high-frequency dispersion step (due to water molecules exchanging on a time scale of a few nanoseconds) is not evident. As a result, it is not possible to resolve the monomer or dimer contribution. Because the samples were apparently not deoxygenated, the analysis is further complicated by a dispersion step from paramagnetic O_2, which could account for one-third of the observed dispersion at pH 4. Nevertheless, it is clear from the data that a dispersion step corresponding to oligomers substantially larger than a dimer is present at all pH values. This is consistent with our findings for unpurified HEWL.

In a more recent contribution, albeit not focused on self-association, a ^{1}H MRD profile was reported for 3.1 mM HEWL at 25 °C without added salt (pH not specified).[56] Although the data extend only to 50 MHz, they are of higher accuracy than those in the earlier study and can therefore be fitted to three correlation times. The quoted correlation times (1.7, 17.5, and 152 ns) appear to be consistent (no errors were given) with the ones obtained here.

Conclusions

The present study demonstrates that the dimerization of a protein as small as HEWL (14.3 kDa) can be conveniently studied by ^{1}H magnetic relaxation dispersion. At 300 K and 5.5 mM HEWL, we find that the protein is monomeric at pH 4 and dimeric at pH 9. This was also found in the earliest studies of HEWL self-association,[27,28] but subsequent work has produced divergent conclusions. The experimentally determined rotational correlation time of the dimer agrees quantitatively with that of a dimer present in 28 tetragonal crystal structures of HEWL. Whether this crystal dimer is also present in solution remains an open question.

The MRD data show, for the first time, that HEWL dimerizes also at pH 4 in the presence of 0.3 M K_2SO_4. This contrasts with a recent dynamic light scattering study,[30] where it was concluded that HEWL remains monomeric even in 1 M $(NH_4)_2SO_4$. In the presence of salt, the MRD data also reveal a higher oligomer with a rotational correlation time corresponding to about 16 HEWL monomers. While we cannot exclude a modest polydispersity in this high-oligomer fraction, a significant (>1%) population of much larger aggregates is ruled out. This higher HEWL oligomer may be identical to the large oligomers inferred from small-angle X-ray scattering on 0.5 M $(NH_4)_2SO_4$ solutions.[37]

The MRD data show that addition of a zwitterionic sulfobetaine suppresses the formation of the higher HEWL oligomer. This finding provides a molecular basis for the observation that sulfobetaines promote crystallization, rather than amorphous precipitation, of HEWL from sulfate solutions.[16] Commercial HEWL preparations are known to contain significant amounts of contaminating proteins, which have been shown to interfere with crystal growth.[44] This observation can be explained by our finding that removal of the contaminating proteins reduces the amount of higher oligomers.

The ^{1}H MRD data presented here, which extend to higher frequencies than previous MRD studies of HEWL, reveal the presence of several protein-associated water molecules with a residence time of about 2 ns at 300 K. This prompted us to reinterpret earlier ^{17}O MRD data,[57] which then indicate that only one of the five buried water molecules in HEWL has a residence time longer than 10 ns at 300 K. The present ^{1}H MRD data suggest that the 2 ns residence time mainly reflects the cluster of four water molecules at the interface of the α and β subunits of HEWL. This assignment is consistent with recent MD simulations.[71]

Acknowledgment. We thank Hans Lilja and Vladimir Denisov for spectrometer assistance, Eva Thulin for advice on protein purification, and Hanna Nilsson for protein purification and characterization. This work was supported by the Swedish Research Council and the Crafoord Foundation.

References and Notes

(1) De Young, L.; Fink, A. L.; Dill, K. A. *Acc. Chem. Res.* **1993**, *26*, 614−620.
(2) Elcock, A. H.; Sept, D.; McCammon, J. A. *J. Phys. Chem. B* **2001**, *105*, 1504−1518.
(3) Minton, A. P. *Curr. Opin. Struct. Biol.* **2000**, *10*, 34−39.
(4) Ellis, R. J. *Curr. Opin. Struct. Biol.* **2001**, *11*, 114−119.
(5) Dobson, C. M. *Trends Biochem. Sci.* **1999**, *9*, 329−332.
(6) Rosenberger, F.; Vekilov, P. G.; Muschol, M.; Thomas, B. R. *J. Cryst. Growth* **1996**, *168*, 1−27.
(7) Riès-Kautt, M.; Ducruix, A. *Methods Enzymol.* **1997**, *276*, 23−59.
(8) Leckband, D.; Israelachvili, J. *Q. Rev. Biophys.* **2001**, *34*, 105−267.
(9) Carlsson, F.; Malmsten, M.; Linse, P. *J. Phys. Chem. B* **2001**, *105*, 12189−12195.
(10) Allahyarov, E.; Löwen, H.; Louis, A. A.; Hansen, J. P. *Europhys. Lett.* **2002**, *57*, 731−737.
(11) Neal, B. L.; Asthagiri, D.; Lenhoff, A. M. *Biophys. J.* **1998**, *75*, 2469−2477.
(12) Curtis, R. A.; Steinbrecher, C.; Heinemann, M.; Blanch, H. W.; Prausnitz, J. M. *Biophys. Chem.* **2002**, *98*, 249−265.

(13) Riès-Kautt, M. M.; Ducruix, A. F. *J. Biol. Chem.* **1989**, *264*, 745−748.
(14) Riès-Kautt, M.; Ducruix, A.; van Dorsselaer, A. *Acta Crystallogr., Sect. D* **1994**, *50*, 366−369.
(15) Forsythe, E. L.; Snell, E. H.; Malone, C. C.; Pusey, M. L. *J. Cryst. Growth* **1999**, *196*, 332−343.
(16) Vuillard, L.; Rabilloud, T.; Leberman, R.; Berthet-Colominas, C.; Cusack, S. *FEBS Lett.* **1994**, *353*, 294−296.
(17) Moretti, J. J.; Sandler, S. I.; Lenhoff, A. M. *Biotechnol. Bioeng.* **2000**, *70*, 498−506.
(18) Taratuta, V. G.; Holschbach, A.; Thurston, G. M.; Blankschtein, D.; Benedek, G. B. *J. Phys. Chem.* **1990**, *94*, 2140−2144.
(19) Broide, M. L.; Tominc, T. M.; Saxowsky, M. D. *Phys. Rev. E* **1996**, *53*, 6325−6335.
(20) Muschol, M.; Rosenberger, F. *J. Chem. Phys.* **1997**, *107*, 1953−1962.
(21) George, A.; Wilson, W. W. *Acta Crystallogr., Sect. D* **1994**, *50*, 361−365.
(22) ten Wolde, P. R.; Frenkel, D. *Science* **1997**, *277*, 1975−1978.
(23) Pusey, M. L.; Nadarajah, A. *Cryst. Growth Des.* **2002**, *2*, 475−483.
(24) Hamiaux, C.; Pérez, J.; Prangé, T.; Veesler, S.; Riès-Kautt, M.; Vachette, P. *J. Mol. Biol.* **2000**, *297*, 697−712.
(25) Gottschalk, M.; Venu, K.; Halle, B. *Biophys. J.* **2003**, *84*, 3941−3958.
(26) Janin, J.; Rodier, F. *Proteins* **1995**, *23*, 580−587.
(27) Sophianopoulos, A. J.; van Holde, K. E. *J. Biol. Chem.* **1964**, *239*, 2516−2524.
(28) Bruzzesi, M. R.; Chiancone, E.; Antonini, E. *Biochemistry* **1965**, *4*, 1796−1800.
(29) Muschol, M.; Rosenberger, F. *J. Chem. Phys.* **1995**, *103*, 10424−10432.
(30) Kuehner, D. E.; Heyer, C.; Rämsch, C.; Fornefeld, U. M.; Blanch, H. W.; Prausnitz, J. M. *Biophys. J.* **1997**, *73*, 3211−3224.
(31) Georgalis, Y.; Umbach, P.; Raptis, J.; Saenger, W. *Acta Crystallogr., Sect. D* **1997**, *53*, 691−702.
(32) Georgalis, Y.; Umbach, P.; Zielenkiewicz, A.; Utzig, E.; Zielenkiewicz, W.; Zielenkiewicz, P.; Saenger, W. *J. Am. Chem. Soc.* **1997**, *119*, 11959−11965.
(33) Velev, O. D.; Kaler, E. W.; Lenhoff, A. M. *Biophys. J.* **1998**, *75*, 2682−2697.
(34) Boué, F.; Lefaucheux, F.; Robert, M. C.; Rosenman, I. *J. Cryst. Growth* **1993**, *133*, 246−254.
(35) Minezaki, Y.; Niimura, N.; Ataka, M.; Katsura, T. *Biophys. Chem.* **1996**, *58*, 355−363.
(36) Seth, E.; Aswal, V. K. *J. Macromol. Sci. B* **2002**, *41*, 77−83.
(37) Ducruix, A.; Guilloteau, J. P.; Riès-Kautt, M.; Tardieu, A. *J. Cryst. Growth* **1996**, *168*, 28−39.
(38) Finet, S., Bonneté, F.; Frouin, J.; Provost, K.; Tardieu, A. *Eur. Biophys. J.* **1998**, *27*, 263−271.
(39) Wilson, L. J.; Adcock-Downey, L.; Pusey, M. L. *Biophys. J.* **1996**, *71*, 2123−2129.
(40) Nesmelova, I. V.; Fedotov, V. D. *Biochim. Biophys. Acta* **1998**, *1383*, 311−316.
(41) Price, W. S.; Tsuchiya, F.; Arata, Y. *J. Am. Chem. Soc.* **1999**, *121*, 11503−11512.
(42) Price, W. S.; Tsuchiya, F.; Arata, Y. *Biophys. J.* **2001**, *80*, 1585−1590.
(43) Muschol, M.; Rosenberger, F. *J. Cryst. Growth* **1996**, *167*, 738−747.
(44) Thomas, B. R.; Vekilov, P. G.; Rosenberger, F. *Acta Crystallogr., Sect. D* **1996**, *52*, 776−784.
(45) Dubin, S. B.; Clark, N. A.; Benedek, G. B. *J. Chem. Phys.* **1971**, *54*, 5158−5164.
(46) Buck, M.; Boyd, J.; Redfield, C.; MacKenzie, D. A.; Jeenes, D. J.; Archer, D. B.; Dobson, C. M. *Biochemistry* **1995**, *34*, 4041−4055.
(47) Pan, B.; Berglund, K. A. *J. Cryst. Growth* **1997**, *171*, 226−235.
(48) Halle, B., Denisov, V. P.; Venu, K. Multinuclear relaxation dispersion studies of protein hydration. In *Biological Magnetic Resonance*; Krishna, N. R., Berliner, L. J., Eds.; Kluwer Academic/Plenum: New York, 1999; pp 419−484.
(49) Halle, B.; Denisov, V. P. *Methods Enzymol.* **2001**, *338*, 178−201.
(50) Gottschalk, M.; Nilsson, H.; Roos, H.; Halle, B. *Protein Sci.*, in press.
(51) Koenig, S. H.; Hallenga, K.; Shporer, M. *Proc. Natl. Acad. Sci. U.S.A.* **1975**, *72*, 2667−2671.
(52) Hallenga, K.; Koenig, S. H. *Biochemistry* **1976**, *15*, 4255−4256.
(53) Bryant, R. G.; Jarvis, M. *J. Phys. Chem.* **1984**, *88*, 1323−1324.
(54) Raeymaekers, H. H.; Eisendrath, H.; Verbeken, A.; van Haverbeke, Y.; Muller, R. N. *J. Magn. Reson.* **1989**, *85*, 421−425.
(55) Kakule, J. F.; Weglarz, W. P.; Shenoy, R. K.; Sharp, A. R.; Peemoeller, H. *Acta Phys. Pol., A* **2000**, *98*, 131−152.
(56) Bertini, I.; Fragai, M.; Luchinat, C.; Parigi, G. *Magn. Reson. Chem.* **2000**, *38*, 543−550.
(57) Denisov, V. P.; Halle, B. *Faraday Discuss.* **1996**, *103*, 227−244.
(58) Denisov, V. P.; Jonsson, B.-H.; Halle, B. *Nat. Struct. Biol.* **1999**, *6*, 253−260.
(59) Halle, B.; Jóhannesson, H.; Venu, K. *J. Magn. Reson.* **1998**, *135*, 1−13.
(60) Hindman, J. C.; Svirmickas, A.; Wood, M. *J. Chem. Phys.* **1973**, *59*, 1517−1522.
(61) Halle, B. Water in biological systems. In *Hydration Processes in Biology*; Bellisent-Funel, M.-C., Ed.; IOS Press: Amsterdam: 1999; pp 233−249.
(62) Wiesner, S.; Kurian, E.; Prendergast, F. G.; Halle, B. *J. Mol. Biol.* **1999**, *286*, 233−246.
(63) Venu, K.; Denisov, V. P.; Halle, B. *J. Am. Chem. Soc.* **1997**, *119*, 3122−3134.
(64) Press, W. H.; Teukolsky, S. A.; Vetterling, W. T.; Flannery, B. P. *Numerical Recipes in C*, 2nd ed.; Cambridge University Press: Cambridge, 1992.
(65) García de la Torre, J.; Huertas, M. L.; Carrasco, B. *Biophys. J.* **2000**, *78*, 719−730.
(66) García de la Torre, J.; Bloomfield, V. A. *Q. Rev. Biophys.* **1981**, *14*, 81−139.
(67) Kuramitsu, S.; Hamaguchi, K. *J. Biochem.* **1980**, *87*, 1215−1219.
(68) Bartik, K.; Redfield, C.; Dobson, C. M. *Biophys. J.* **1994**, *66*, 1180−1184.
(69) Denisov, V. P.; Halle, B. *J. Am. Chem. Soc.* **2002**, *124*, 10264−10265.
(70) Vaney, M. C.; Maignan, S.; Riès-Kautt, M.; Ducruix, A. *Acta Crystallogr., Sect. D* **1996**, *52*, 505−517.
(71) Sterpone, F.; Ceccarelli, M.; Marchi, M. *J. Mol. Biol.* **2001**, *311*, 409−419.
(72) Denisov, V. P.; Halle, B. *J. Mol. Biol.* **1995**, *245*, 698−709.
(73) Marchi, M.; Sterpone, F.; Ceccarelli, M. *J. Am. Chem. Soc.* **2002**, *124*, 6787−6791.
(74) Wills, P. R.; Nichol, L. W.; Siezen, R. J. *Biophys. Chem.* **1980**, *11*, 71−82.
(75) Legrand, L.; Rosenman, I.; Boué, F.; Robert, M.-C. *J. Cryst. Growth* **2001**, *232*, 244−249.
(76) Vuillard, L.; Rabilloud, T.; Goldberg, M. E. *Eur. J. Biochem.* **1998**, *256*, 128−135.
(77) Nicholls, A.; Sharp, K. A.; Honig, B. *Proteins* **1991**, *11*, 281−296.